SPACECRAFT MAGNETIC CLEANLINESS PREDICTION AND CONTROL

S.Weikert[1], **K.Mehlem**[2], **A.Wiegand**[1]

[(1)] Astos Solution GmbH, Stuttgart, Germany, [(2)] ESA (Retired)

ABSTRACT

The paper describes a sophisticated and realistic control and prediction method for the magnetic cleanliness of spacecraft, covering all phases of a project till the final system test. From the first establishment of the so-called magnetic moment allocation list the necessary boom length can be determined. The list is then continuously updated by real unit test results with the goal to ensure that the magnetic cleanliness budget is not exceeded at a given probability level. A complete example is described. The synthetic spacecraft modeling which predicts only quite late the final magnetic state of the spacecraft is also described. Finally, the most important cleanliness verification, the spacecraft system test, is described shortly with an example. The emphasis of the paper is put on the magnetic dipole moment allocation method.

1. BOOM LENGTH DESIGN

A spacecraft has many magnetic parts. A minority of these parts, like travelling wave tubes, batteries, thrusters, experiments etc., called culprits, consume the major part of the magnetic cleanliness budget. Therefore booms are used to place the magnetometer sensor at save distance from the spacecraft. Their length can vary from 1 to about 11 m.

This length is a critical design element and it has to be determined on the basis of global moment estimations of the magnetic parts.

The necessary boom length is found when the total field of all units at the boom tip does not exceed the magnetic cleanliness budget at a given probability level.

The field at the boom tip is given by (vectors in small bold, matrices in capital bold):

$$\mathbf{b}(\tau) = \sum_{i=1}^{n} \frac{3\cdot\left[\Delta\mathbf{r}_i\cdot\Delta\mathbf{r}_i^{\,T} - |\Delta\mathbf{r}_i|^2\cdot\mathbf{I}\right]}{|\Delta\mathbf{r}_i|^5}\cdot|\mathbf{m}_i|\cdot\mathbf{R}_i\cdot\mathbf{e} \qquad (1)$$

with
$$\Delta\mathbf{r}_i = (\tau\cdot\mathbf{r}^{sp\,0} - \mathbf{r}_i) \qquad (2)$$

where $\mathbf{r}_0^{sp}$ is the initial guess of the position of the boom tip, $\mathbf{r}_i$ are the centers of the units and τ is the boom length correction factor. $\mathbf{R}_i$ are the random matrices of the allocated unit moments $|\mathbf{m}|_i$, $\mathbf{e}^T=\frac{1}{\sqrt{3}}[111]$ is the unit vector and $\mathbf{I}$ is the unity matrix. The index ^{sp} stands for specification point.

Through a Monte-Carlo simulation starting with $\tau^0=1$ and $\mathbf{r}^{sp\,0}$ as a suitable initial guess, the 3σ field at the boom tip is determined by random variations of the unknown directions and moments. The end points of the random vectors $\mathbf{R}_i\cdot\mathbf{e}$ have to be distributed uniformly on a sphere.

At the start an error ε^0 between the field module $|\mathbf{b}^{sp\,0}(\tau^0)|$ and the cleanliness specification b^{sp} will be observed:

$$\varepsilon^0(\tau^0,\mathbf{r}^{sp\,0}) = |\mathbf{b}^{sp\,0}(\tau^0,\mathbf{r}^{sp\,0})| - b^{sp} \qquad (3)$$

By use of a one-dimensional search on the boom length correction factor τ its optimal value of is found when:

$$\tau = \tau^{opt} \text{ if } \varepsilon(\tau, \mathbf{r}^{sp\,0}) = 0 \qquad (4)$$

The optimal position of the boom tip is then:

$$\mathbf{r}^{sp\,opt} = \tau^{opt}\cdot\mathbf{r}^{sp\,0} \qquad (5)$$

Or if the boom root $\mathbf{r}^{root}$ is chosen, the optimal boom length L becomes:

$$L^{opt} = |\mathbf{r}^{sp\,opt} - \mathbf{r}^{root}| \qquad (6)$$

The DIMAL software, containing this algorithm, allows to perform easily parametric scans by varying the moment allocations and the probability levels, as will be explained in §2.

2. MOMENT ALLOCATION METHOD

At the start of a project some units are quite well known from previous projects, some major contributors have to be identified by magnetic sniffing, and the rest has to be estimated by the moment allocation method.

In the following phases of the project more and more units become available for magnetic testing and for the determination of their MDM (Multiple Dipole Model [1]). In the budgeting process for unknown units only the global dipole moment vectors are considered. Their moment allocations are optimized in order to fit the field budget.

A magnetic review board would analyze the list frequently. In such a way early warnings arise when some units exceed the budget. Thereupon corrective actions can be defined, whether by changing critical ferro-magnetic parts or electrical design (loops). When the involved units cannot be corrected for instance a magnetic compensation by magnets can be applied, as has been done for the Ulysses Travelling Wave Tubes and the Radioisotope Thermal Power Generator (RTG).

Proc. '2012 ESA Workshop on Aerospace EMC', Venice, Italy, (ESA SP-702, May 2012)

In exceptional cases shielding with μ-metal can be applied. The allocation list is thus a budget household tool and it evolves throughout the projects development.

The allocation method distinguishes between three categories of units (Fig. 1):

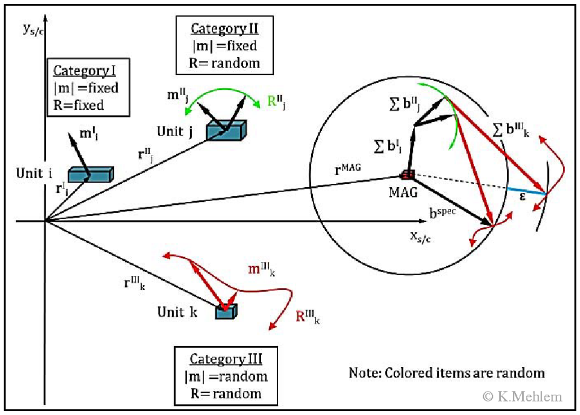

Figure 1. Concept of magnetic moment allocation

The Category I comprises all units or parts which are quite well known from previous projects, like travelling wave tubes or thrusters etc. Their moment vectors are considered as fix.

The Category II comprises all units whose modules of the moments are known from experience, but whose directions are unknown. The directions are then subject of the moment allocation by stochastic evaluation.

Finally the Category III comprises all those units whose moment vectors are completely unknown and which are thus the subject of the moment allocation by stochastic evaluation of both module and direction.

The total Cat. I field is deterministic in both $\mathbf{R}_j^I$ and $|\mathbf{m}|_j^I$:

$$\mathbf{b}^I=\sum_{i=1}^{n^I}\frac{3\cdot\left[(\mathbf{r}^{sp}-\mathbf{r}_i^I)\cdot(\mathbf{r}^{sp}-\mathbf{r}_i^I)^T-\left|\mathbf{r}^{sp}-\mathbf{r}_i^I\right|^2\cdot\mathbf{I}\right]}{|\mathbf{r}^{sp}-\mathbf{r}_i^I|^5}\cdot\mathbf{R}_i^I\cdot\mathbf{m}_i^I \quad (7)$$

The total Cat. II field is deterministic in $|\mathbf{m}|_j^{II}$ and random in $\mathbf{R}_j^{II}$:

$$\mathbf{b}^{II}=\sum_{i=1}^{n^I}\frac{3\cdot\left[(\mathbf{r}^{sp}-\mathbf{r}_i^{II})\cdot(\mathbf{r}^{sp}-\mathbf{r}_i^{II})^T-\left|\mathbf{r}^{sp}-\mathbf{r}_i^{II}\right|^2\cdot\mathbf{I}\right]}{|\mathbf{r}^{sp}-\mathbf{r}_i^{II}|^5}\cdot|\mathbf{m}_i^{II}|\cdot\mathbf{R}_i^{II}\cdot\mathbf{e} \quad (8)$$

The total Cat. III field is both random in $|\mathbf{m}|_j^{III}$ and in $\mathbf{R}_j^{III}$:

$$\mathbf{b}^{III}=\sum_{k=1}^{n^{III}}\frac{3\cdot\left[(\mathbf{r}^{sp}-\mathbf{r}_k^{III})\cdot(\mathbf{r}^{sp}-\mathbf{r}_k^{III})^T-\left|\mathbf{r}^{sp}-\mathbf{r}_k^{III}\right|^2\cdot\mathbf{I}\right]}{|\mathbf{r}^{sp}-\mathbf{r}_k^{III}|^5}\cdot\lambda\cdot|\mathbf{m}|_j^{III}\cdot\mathbf{R}_k^{III}\cdot\mathbf{e}$$

(9)

where λ is the moment adjustment factor.

Its optimal value λ^{opt} is reached when the 3σ budget constraint is satisfied (see also Eqs. 3 and 4):

$$\lambda=\lambda^{opt}\text{ if }\left|\mathbf{b}^I+\mathbf{b}^{II}+\lambda\cdot\sum_{k=1}^{n^{III}}\mathbf{b}_k^{III}\right|_{3\sigma}=b^{sp} \quad (10)$$

The equal field repartition for Cat. III fields is:

$$|\mathbf{b}_k^{III}|=\frac{|\mathbf{b}^{III}|}{n^{III}} \quad (11)$$

Since the Cat. III units are of course located at different positions r_k^{III} this translates into an unequal moment repartition:

$$|\mathbf{m}|_k^{III}(\mathbf{r}_k^{III})=\frac{|\mathbf{b}^{III}|\cdot|\mathbf{r}^{sp}-\mathbf{r}_k^{III}|^3}{2\cdot n^{III}} \quad (12)$$

The result of this strategy is that units close to the specification point have a lower moment allowance than more remote units.

In the allocation process the end points of the vectors $\mathbf{R}_i\cdot\mathbf{e}$ are uniformly distributed on a sphere, whereas the non-fixed moments are defined by the equal field repartition (Eq. 12). The initial guess for the moments is calculated from Eq. 11 which implies the highly improbable assumption that each Cat. III moment vector points in the direction of the specification point (first Gauss position). Thereupon the 3 different parts of the total field (Eq. 7 to 9) are calculated. Whereas the Cat. I field $\mathbf{b}^I$ is deterministic, the Cat. II and III 3σ fields $\mathbf{b}^{II}$ **and** $\mathbf{b}^{III}$ are determined by random variations of the unknown directions and moments.

At the start an error ε^0 will be observed: (see Fig. 1):

$$\varepsilon^0\neq b^{sp}-\left|\mathbf{b}^I+\mathbf{b}^{II}+\lambda^0\cdot\sum_{k=1}^{n^{III}}\mathbf{b}_k^{III}\right|_{3\sigma} \quad (13)$$

The moment adjustment factor λ appears in Eq. 9 and 13. By use of a one-dimensional search on the moment adjustment factor λ its optimal value of is found when Eq. 10 is satisfied. And so are the optimal allocated Cat. III moments $|\mathbf{m}|_k^{III\,opt}$ (see Fig. 2):

$$|\mathbf{m}|_k^{III\,opt}=\lambda^{opt}\,|\mathbf{m}|_k^{III} \qquad k=1,n^{III} \quad (14)$$

The Fig. 2 shows a shortened allocation list (output of the DIMAL software) which can contain over 100 units for a spacecraft. The total field budget is 25nT. The number of Monte-Carlo runs is 20000. The probability level is set to 3σ and the associated total field module turns out to be 25.1nT, thus very close to the budget.

__Input:__
Total allocated field at MAG-location [nT] = 25.
MAG-location [cm] in S/C frame = -225.0 75.0 33.9
Number of trials = 20000
Number of classes = 200
Confidence level [%] = 3σ

__Legend of Output:__
x,y,z = unit coordinates in S/C frame [cm]
r = distance between unit and MAG-location [cm]
b = field of unit at MAG [nT] (FGP)
m = unit moment [$Gcm^3 = 10^{-3}Am^2 = mAm^2$] = max.allocation
CAT I = known moment and unknown direction
Cat II = unknown direction of known moment
Cat III = unknown moment and unknown direction
FGP = First Gaussian Position

Unit	x	y	z	r	b	m	.
PDU P/L	29.1	-86.0	198.7	343.	0.0	10.	Cat II
PDU S/S	-68.7	-86.0	71.6	228.	0.2	10.	Cat II
BCU	56.0	-91.0	41.0	326.	2.1	366.	Cat III
Battery 1	86.5	-91.2	49.5	353.	0.0	10.	Cat II
Battery 2	86.5	-91.2	83.0	356.	0.0	10.	Cat II
Battery 3	61.0	-91.2	83.0	334.	0.1	10.	Cat II
SADM_+y	0.0	91.1	132.0	246.	0.3	20.	Cat II
SADM_-y	0.0	-91.1	132.0	296.	0.2	20.	Cat II
SADE	-21.5	-89.2	30.5	262.	0.1	10.	Cat II
Solar Array -y_1	0.0	-359.7	132.0	499.	0.2	125.	Cat I
Solar Array -y_2	0.0	-644.5	132.0	760.	0.1	125.	Cat I
Solar Array -y 3	0.0	-929.3	132.0	1034.	0.0	125.	Cat I
			⋮				
WDE	59.3	90.5	83.0	289.	0.1	10.	Cat II
RW1	75.0	20.0	130.0	320.	2.1	344.	Cat III
RW2	75.0	20.0	90.0	310.	2.1	314.	Cat III
RW3	75.0	-20.0	130.0	329.	2.1	375.	Cat III
RW4	75.0	-20.0	90.0	320.	2.1	344.	Cat III
Gyro Unit 1	-20.0	-90.5	58.8	265.	2.1	195.	Cat III
Gyro Unit 2	-20.0	-90.5	83.8	268.	2.1	203.	Cat III
Gyro Unit 3 - tbd	0.0	0.0	0.0	240.	2.1	145.	Cat III
			⋮				

__Fields at MAG location:__
Field from Cat I moments = 0.6 nT
Field from Cat I+Cat II moments (FGP) = 7.2 nT
Field from Cat I+Cat II moments (50%) = 1.8 nT
Field from Cat III moments (FGP) = 106.4 nT
Field from Cat II+Cat III moments (FGP) = 113.3 nT
Worst case field from all moments (FGP) = 113.9 nT
Total field allocation (Spec) = __25.0__ nT
Total field at 99.50% confidence level = __25.1__ nT

Figure 2. Typical moment allocation list (red items) for satisfaction of the budget constraint at 3σ

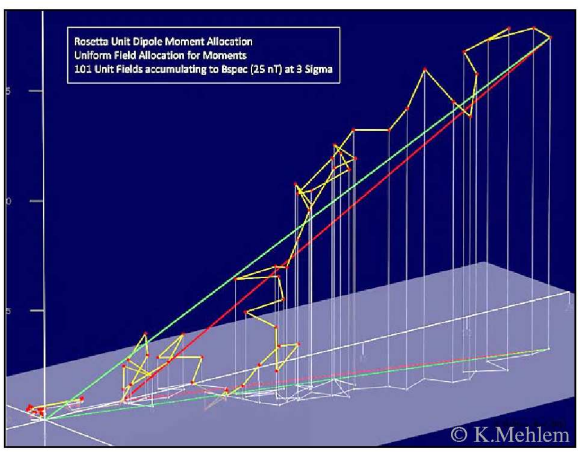

Figure. 3. Example of a compliant field vector combination (3σ)

The Fig. 3 shows one possible 3σ example of individual field vectors (yellow) summing up to the budget (green line).A surprising fact is that the worst case (all moments pointing in the first Gauss position to the specification point) is 113.9nT, thus 4.5 times higher than the 3σ case. This means that the present moment allocation method avoids the disadvantages associated with conventional, more penalizing budgeting.

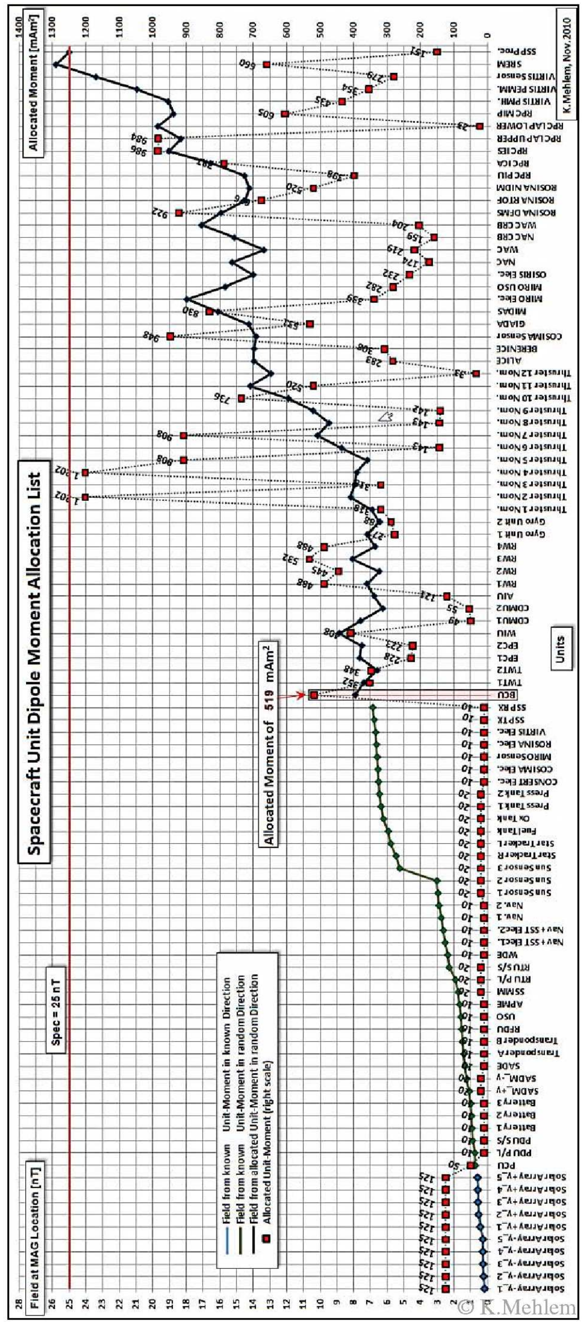

Figure. 4. Example of a compliant field vector combination (3σ) and allocated moments

The Fig. 4 shows the allocated moments $|\mathbf{m}_i|$ (red squares) and a possible 3σ example of individual field vectors $\mathbf{b}_j$. The module of the vector sum including all units from 1 to i is: $\left|\sum_{j=1}^{i} \mathbf{b}_j\right|$. This quantity (green, blue) is growing from the 'left' and reaching the budget at the 'right, top'.

The Fig. 4 represents an example. Also the allocated moments are shown (red squares). As a consequence of the equal-field repartition (Eq. 12) some units have a large moment allocation due to their greater distance from the specification point.

On the Fig. 3 an example drawn from the 20000 3σ solutions is visualized in 3D. The yellow field vectors meet the spec (green line) (see also Fig. 4). The combination of the individual field vectors appears remarkably crumpled compared to the severity of the implied probability. They would stretch out by a factor of more than 4 in the present case.

The allocation method presented is thus a powerful and well controllable simulation tool which is of great value for the engineers dealing with magnetic cleanliness, whether it is the person doing unit tests, who can pull the alarm, or the review board which derives corrective actions.

3. SYNTHETIC SPACECRAFT MODEL

In a complementary activity the unit models after test are integrated into the synthetic spacecraft model via coordinate transformations. The equations of these transformations of a dipole i from the test to the spacecraft frame are (see Fig. 5):

$$\mathbf{M}_i^s = [\mathbf{r}_i^s \quad \mathbf{m}_i^s\,] \tag{15}$$

with
$$\mathbf{r}_i^s = \mathbf{u}_i^s + \mathbf{R}_i^{us} \cdot \mathbf{t}_i^u + \mathbf{R}_i^{us} \cdot \mathbf{R}_i^{tu} \cdot \mathbf{r}_i^t \tag{16}$$

and with
$$\mathbf{m}_i^s = \mathbf{R}_i^{us} \cdot \mathbf{R}_i^{tu} \cdot \mathbf{m}_i^t \tag{17}$$

$\mathbf{R}^{ab}$ is the coordinate rotation matrix leading from frame a to frame b. $\mathbf{r}^t$ is the dipole position in test frame; $\mathbf{t}^u$ is the reference hole of the unit in the unit frame; $\mathbf{u}^s$ is the reference hole of the unit in spacecraft frame; $\mathbf{r}^s$ is finally the dipole position in the spacecraft frame. Much care has to be taken in determining correctly the different rotation matrices $\mathbf{R}^{ab}$.

The synthetic spacecraft model is defined as the collection of all unit MDMs in the array:

$$\mathbf{M}^s = \begin{bmatrix} \mathbf{M}_1^s \\ \vdots \\ \mathbf{M}_i^s \\ \vdots \\ \mathbf{M}_n^s \end{bmatrix} \tag{18}$$

The field at the specification point (boom tip) is then:

$$\mathbf{b}^{sp} = \sum_{i=1}^{n} \frac{3 \cdot \left[(\mathbf{r}^{sp} - \mathbf{r}_i^s) \cdot (\mathbf{r}^{sp} - \mathbf{r}_i^s)^T - |\mathbf{r}^{sp} - \mathbf{r}_i^s|^2 \mathbf{I} \right]}{\left| \mathbf{r}^{sp} - \mathbf{r}_i^s \right|^5} \cdot \mathbf{m}_i^s \tag{19}$$

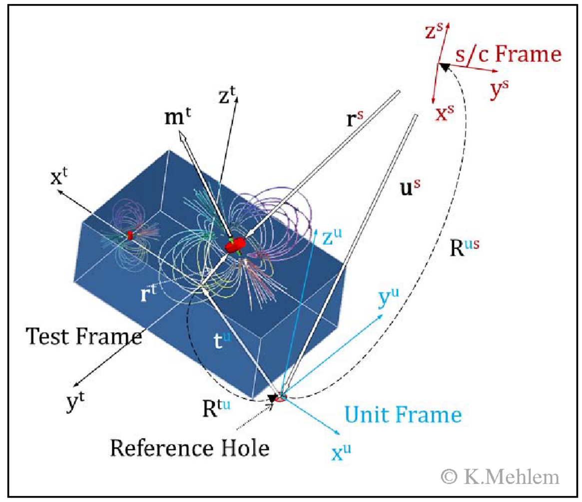

Figure 5. Concept of MDM coordinate transformations

Figure 6. shows an example of units transformed from test frame to spacecraft frame. The different unit models $\mathbf{M}_i^s$ could be visualized as vectors inside each unit box. (Cluster) [3]. The ensemble of these vectors form the synthetic spacecraft model (Eq. 18).

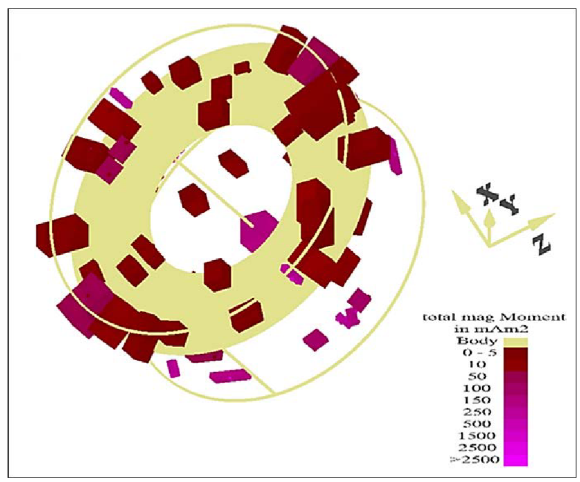

Figure 6. Units assembled in a synthetic spacecraft model (color indicates moment strength) (H.Kuegler)

As already mentioned above the eventual induced magnetic moments in some soft-magnetic materials by neighboring magnetic units on board the spacecraft, together with some possible coordinate transformations errors, can be accountable for large differences (>30%) between the synthetic and the tested MDM, as has been observed in the case of Cluster.

In this respect the manpower-intensive generation of a synthetic spacecraft model versus achievable precision should be subject of a careful trade-off.

4. SPACECRAFT SYSTEM TEST

The ultimate verification of the magnetic cleanliness of a spacecraft is the so-called magnetic system test. As mentioned already, some units on board a spacecraft containing soft-magnetic material, can change their magnetic properties by induced moments from other units. By the magnetic mapping of the fully integrated spacecraft these effects are then included in the spacecraft model.

.First the spacecraft model $\mathbf{M}^s$ is determined by use of a NLP solver as described in [1], and thereupon the field at the specification point is calculated (Eq. 19). If the cleanliness specification is violated one possible technique which has been extensively practiced in the past, could be the compensation of the spacecraft by use of compensation magnets. The magnets are calculated by the following formulas [1]:

($\boldsymbol{D}^{mag+}$ being the pseudo inverse of $\boldsymbol{D}^{mag}$)

$$\boldsymbol{m}^{mag\ opt} = -\boldsymbol{D}^{mag+} \cdot \boldsymbol{D}^{to} \cdot \boldsymbol{m}^{to\ opt} \tag{20}$$

$\boldsymbol{D}^{mag}$ contains the matrices $\mathbf{D}_{ij}^{mag}$:

$$\mathbf{D}_{ij}^{mag} = \frac{3 \cdot \left[\left(\mathbf{r}_i^{sp} - \mathbf{r}_j^{mag}\right) \cdot \left(\mathbf{r}_i^{sp} - \mathbf{r}_j^{mag}\right)^T - \left|\left(\mathbf{r}_i^{sp} - \mathbf{r}_j^{mag}\right)\right|^2 \cdot \mathbf{I} \right]}{\left|\left(\mathbf{r}_i^{sp} - \mathbf{r}_j^{mag}\right)\right|^5} \tag{21}$$

and $\boldsymbol{D}^{to}$ contains the matrices $\mathbf{D}_{ij}^{to}$:

$$\mathbf{D}_{ik}^{to} = \frac{3 \cdot \left[\left(\mathbf{r}_i^{sp} - \mathbf{r}_k^{to}\right) \cdot \left(\mathbf{r}_i^{sp} - \mathbf{r}_k^{to}\right)^T - \left|\left(\mathbf{r}_i^{sp} - \mathbf{r}_k^{to}\right)\right|^2 \cdot \mathbf{I} \right]}{\left|\left(\mathbf{r}_i^{sp} - \mathbf{r}_k^{to}\right)\right|^5} \tag{22}$$

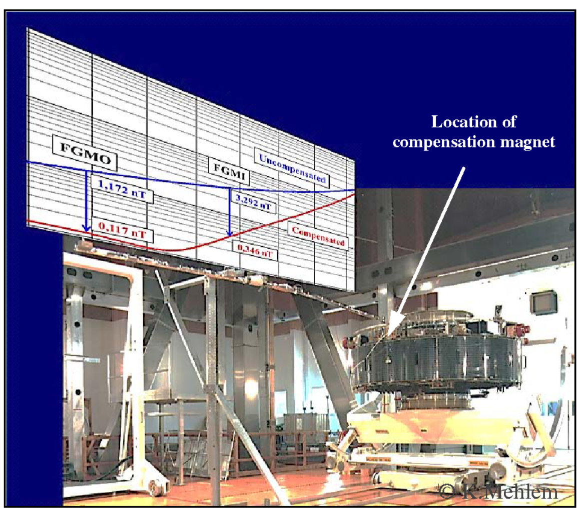

Figure 7. Field compensation at the FGMI and FGMO locations by use of 1 magnet only (photo: ESA/IABG)

An example of using additional magnets for compensation of a spacecraft (Cluster) [2] is shown on the Fig. 7. The white insert shows the fall-off fields along the spacecraft boom, both for the uncompensated and for the compensated state of the spacecraft. In the present case the compensation (red line) was done with only one magnet which means that according to Eq. 20 only a least square fit solution could be obtained. Still, the fields at both magnetometers (FGMI and FGMO) were reduced by about one order of magnitude. The cleanliness specification of 0.25nT was therefore verified with a comfortable margin.

5. CONCLUSION

The magnetic dipole allocation method is a powerful and sophisticated magnetic field budget control tool which allows a justified, tailored magnetic moment allocation also for magnetically unknown units and equipment already in an early stage of a project.

The synthetic spacecraft model is also a possible control tool, however with limited accuracy due to mutual induction effects which cannot be included in the numerical superposition of dipoles.

The ultimate verification of the cleanliness state of a spacecraft is undoubtedly the system test. It delivers the most precise information about the magnetic state of the spacecraft and it allows last-minute corrective action if required, for instance in form of additional hard-magnetic compensation magnets.

6. REFERENCES

1. Mehlem, K., Multiple magnetic dipole modeling and field prediction of satellites, IEEE Transactions on Magnetics, Sep 1978, Vol.14, Issue:5, on pages 1064-1071, ISSN: 0018-9464.

2. Mehlem, K., Magnetic properties of the Cluster I and II spacecraft, 11 ESA/ESTEC Working Papers, 2000.

3. Kuegler, H., Performance Improvement of the Magnetic Field Simulation Facility MFSA, Proceedings of the 5th International Symposium on Environmental Testing for Space Programmes Noordwijk, The Netherlands (ESA SP-558, June 2004).